SUMMARY REPORT

on

SPACE-VEHICLE STABILIZED-PLATFORM GIMBAL-SYSTEM WEIGHT-REDUCTION STUDY

PHASE II. DESIGN OF SPHERICAL GIMBALS

NAS 8-5101

to

GEORGE C. MARSHALL
SPACE FLIGHT CENTER

July 2, 1963

by

J. E. Sorenson, T. J. Atterbury, and G. M. McClure

BATTELLE MEMORIAL INSTITUTE
505 King Avenue
Columbus 1, Ohio

ABSTRACT

A 16841

This report describes the experimental analysis and design of spherical gimbals. The primary objective of this program was to investigate the advantages of using spherical gimbals in place of ring gimbals for the supporting members of a stabilized platform.

A completely experimental approach was used to evaluate this spherical geometry for these members. A test gimbal was fabricated from aluminum and instrumented with strain gages. Various tests were conducted to determine the stresses and deflections that occur under the stimulated operational loading conditions. The resulting data was then used to design the spherical gimbals.

The over-all results of these experiments show that spherical gimbals do not offer any weight saving over the proposed ring design resulting from the work in Phase I of this program. They are, however, lighter in weight than the ring design presently in use. Also, these spherical gimbals are much stiffer than either the present or proposed ring design, resulting in a system resonant frequency which should be in excess of 200 cps.

Author

This research program was initiated in July, 1962, under contract with NASA. This report covers the work performed on Phase II during the period November 1, 1962, to June 30, 1963.

TABLE OF CONTENTS

SPACE-VEHICLE STABILIZED-PLATFORM GIMBAL-SYSTEM WEIGHT-REDUCTION STUDY

PHASE II. DESIGN OF SPHERICAL GIMBALS

by

J. E. Sorenson, T. J. Atterbury, and G. M. McClure

INTRODUCTION

Work on Phase I, "Design of Ring Gimbals", was completed in December, 1962. A summary report covering all the work, results, and recommendations regarding a ring-gimbal system was submitted for approval on December 28, 1962. It was learned in this study that the controlling factor in this design was stiffness, rather than strength, especially in the redundant gimbal. Even with stiffness as the controlling factor, a substantial weight saving was achieved in the ring-gimbal system.

An additional improvement in stiffness and possibly weight may exist with the use of thin spherical shells rather than rings.

This research program was undertaken to investigate the advantage of using thin spherical shells as the supporting members of a stabilized platform.

The initial approach attempted was a semiempirical one. Analytical solutions which cover portions of the shell were put together in order to obtain an understanding of the gross stress picture and approximate values of wall thickness for each of the gimbals. The solutions for stresses thus obtained included important dimensional parameters for translating information gained on one shell to those of different sizes. To obtain these solutions it was necessary to make the assumption that the effect of the flanges (at the junction of the center portion and covers of the gimbal) on the stresses was negligible. It was learned early in the experimental program, however, that these flanges carry a large portion of the load for most loading conditions and therefore have an appreciable effect on both the magnitude and distribution of the stresses in the thinner portions of the gimbal. It was, as a result, decided to use a completely experimental approach.

Experiments were then carried out on one particular shell, the redundant gimbal, obtaining experimental data relating stresses to inertial loads. These results were then analyzed to determine possible modifications to minimize the weight without appreciably decreasing the stiffness. After the design for the redundant gimbal was completed, the results were then interpreted to apply to other gimbals.

Included in this design was a materials-selection study. Various materials were considered for strength, stiffness, minimum weight, dimensional stability, and fabricability.

RESULTS, RECOMMENDATIONS, AND CONCLUSIONS

The experimental results show that the stresses for an 8-g inertial load are very low. On the basis of strength, this indicates that a substantial reduction in the thickness of the test gimbal can occur without increasing the stresses above allowable values. Considering only strength, the thickness of the shells is sufficiently small that they become very difficult to fabricate to required tolerances. Also, the stiffness of the center portion should be such that the displacements for a 1-g static load with the spherical covers removed will be small. This is important to minimize possible misalignments during repeated assembly and disassembly.

The experimental results also indicated that the flanges carried a relatively large portion of the load. In order to take advantage of this fact, the center section, including the flanges, should be designed to support a major portion of the load.

On the basis of the experimental results, the following recommendations are made:

(1) Considering the stiffness and fabricability requirements, it is believed desirable to limit the minimum thickness to 0.040 inch for the spherical covers and 0.060 inch for the center section.

(2) In order to increase the stiffness of the center section in the most economical fashion, a larger fillet radius should be used at the junction of the flange and center section. Another advantage is that this larger fillet radius reduces the stress concentration normally found in these sharp re-entrant corners.

(3) The cutout in the covers should be made in the spherical portion, leaving the cover flange intact. This will minimize misalignments between the covers and center section while retaining some of the loss in stiffness resulting from the cutout. Sharp re-entrant corners should be avoided at the spherical cover flange.

(4) In order to maintain the continuity of the spherical geometry, not less than 20 fasteners (18-degree spacing) should be used to attach each cover to the center section.

The design resulting from the experimental analysis and the additional considerations mentioned above is summarized in Figure 1 and Table 1. Figure 1 is a cross-section of the three gimbals showing the important dimensions. Table 1 shows the basic dimensions and estimated weight of the three gimbals. The reduction in the weight resulting from holes which may be added to the spherical covers is not included. This may result in a 10 to 15 per cent reduction in the estimated weights shown.

The primary conclusion resulting from this study is that it appears that spherical gimbals do not offer a weight saving over the proposed ring design which resulted from the work in Phase I. They are, however, lighter in weight than the ring gimbals presently being used. The principal advantage appears to be in the much-increased stiffness. The spherical gimbals will be much stiffer than either the present ring gimbals

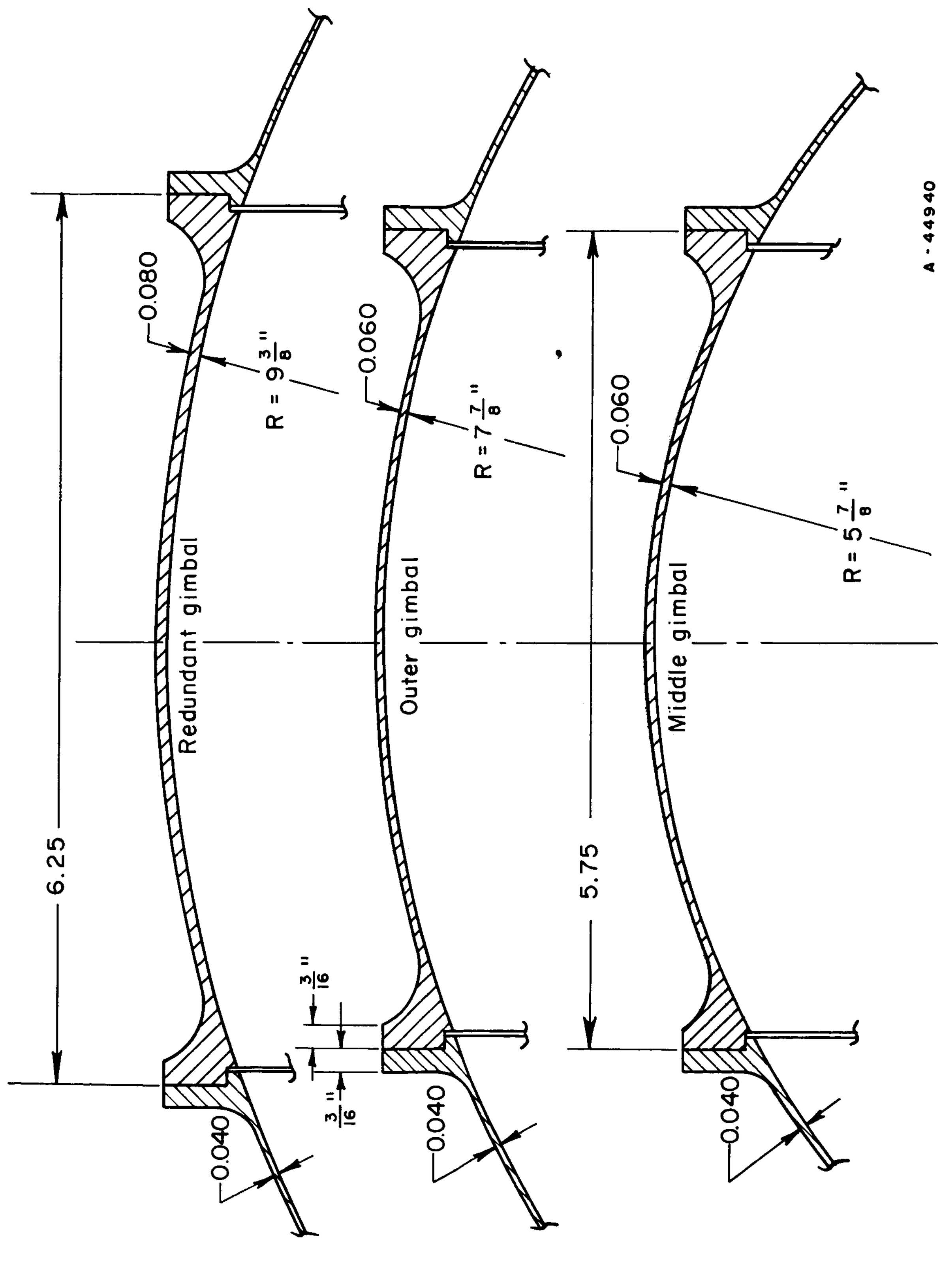

FIGURE 1. CROSS SECTION OF PROPOSED SPHERICAL GIMBAL DESIGN

or the proposed ring design, regardless of what material is used. If, however, fabrication of these shells from beryllium proves feasible, they would weigh slightly more than the proposed ring design and would be considerably stiffer. With beryllium spherical gimbals, the lowest response frequency of the system would probably increase to a value in excess of 200 cps.

TABLE 1. BASIC DIMENSIONS AND ESTIMATED WEIGHTS OF THE SPHERICAL GIMBALS

Gimbal		Thickness of Center Section, inch	Thickness of Cover, inch	Spherical-Gimbal Estimated Weight, pounds	Weight of Proposed Rings, pounds	Weight of Present Rings, pounds
	Be	0.060	0.040	3.66	3.02	7.93
Middle	Al	0.060	0.040	5.46	--	--
	Mg	0.080	0.060	3.90	--	--
	Be	0.060	0.040	4.95	2.65	5.96
Outer	Al	0.060	0.040	7.39	--	--
	Mg	0.080	0.060	5.56	--	--
	Be	0.080	0.040	6.75	5.44	12.30
Redundant	Al	0.080	0.040	10.10	--	--
	Mg	0.100	0.060	7.64	--	--
	Be	--	--	15.36	11.11	26.19
Totals	Al	--	--	22.95	--	--
	Mg	--	--	17.10	--	--

An Alternative Design

Because the stiffness of the redundant gimbal in the ring system appears to control the response frequency of the system, an alternative possibility is to use the spherical geometry for this gimbal but retain the ring geometry for the outer and middle gimbals. One of the reasons for the increased weight of the spherical gimbal assembly is the arrangement of the system. In the ring system, the outer gimbal was smaller in diameter than the middle gimbal, resulting in limits on the rotation about one of the axis. In the spherical-gimbal assembly, the outer gimbal must be larger in diameter than the middle gimbal, resulting in a slight increase in weight simply due to the arrangement. The weight of this alternative assembly (spherical redundant gimbal with rings for the outer and middle gimbals) will be approximately the same as the proposed ring gimbal assembly (assuming beryllium can be used for the spherical redundant gimbal), but the system response frequency should be in excess of 200 cps.

MATERIAL SELECTION

The selection of an optimum material or combination of materials for construction of the spherical-gimbal assembly was based primarily on the following considerations (in the approximate order of importance):

(1) Stiffness

(2) Dimensional stability

(3) Weight

(4) Strength

(5) Fabricability.

The gimbals must have sufficient stiffness so that deflections and vibrations are kept within the design values. The weight of the assembly should be a minimum. For the purpose of material selection, it is convenient to use the recommended minimum thicknesses and a comparison of the properties of the various materials made on this basis.

Stiffness should be a maximum value. This can be assumed to vary proportionately with Et^3 (where E is the elastic modulus in tension, and t is the nominal wall thickness of the spheres).

Dimensional stability requires that the material be metallurgically stable at ambient temperatures (for example, significant aging should not occur during storage or service) and that the strength be sufficiently high to prevent yielding of the material during periods of high acceleration.

Fabricability takes into account the ability of the material to be fabricated into the desired shape by casting, machining, forming, welding, or some combination of these processes.

These considerations are reviewed for a number of potential materials in Table 2. On the basis of stiffness, beryllium appears to be about twice as good as magnesium, and about four times better than aluminum. On a strength basis, it is comparable to magnesium and inferior to wrought aluminum, but considered adequate for the intended application.

Problems encountered in the fabrication of beryllium are considered serious, and the only method presently considered feasible for the intended application is machining from hot-pressed block. However, in the near future, using the gas-pressure bonding technique, it may be possible to form these spheres directly to approximate size from beryllium. Serious fabricational difficulties are not anticipated with the other materials.

If it becomes feasible to fabricate these spherical shapes from beryllium, this would be the first choice for the material because of its exceptionally high stiffness. The center portion of the spherical gimbals could still be machined from hot-pressed block.

TABLE 2. PROPERTIES OF ALTERNATIVE MATERIALS

	Beryllium		Magnesium				Aluminum	
Alloy(a)	Better than 2 per cent BeO	Better than 2 per cent BeO	AZ31B-H24	AZ80A-T5	ZK60A-T5	QE22A-T6	7075-T6	356-T61
Form	Hot-pressed block	Sheet and plate	Sheet and plate	Forging	Forging	Casting	Sheet and plate	Casting
Specification	AMS-7901	AMS-7902	QQ-M-44	QQ-M-40	QQ-M-40	--	QQ-A-283	QQ-4-601
Density, lb/in.^{3}	0.067	0.067	0.064	0.065	0.066	0.065	0.101	0.097
Thickness, in.	0.040	0.040	0.060	0.060	0.060	0.060	0.040	0.040
Elastic Modulus, 10^6 psi	42.5	43.5	6.5	6.5	6.5	6.5	10.3	10.3
Stiffness, in-lb	2720	2790	1405	1405	1405	1405	660	660
Minimum Tensile Yield Strength, psi	30,000	45,000	29,000	28,000	26,000	25,000	66,000	20,000
Section Strength, lb/in.	1200	1800	1740	1680	1560	1500	2600	800
Stiffness/Weight $\left(\frac{E\,t^3}{\rho}\right) \times 10^3$	40.6	41.6	22.0	21.6	21.3	21.6	6.5	6.8
Fabricability Considerations	Forming extremely difficult; weldability very poor; must be machined from block; ductility poor	Forming extremely difficult; weldability very poor; must be machined from block; sheet anisotropic	Good; welds should be stress relieved to prevent stress-corrosion cracking	Good; welds should be stress relieved to prevent stress-corrosion cracking	Good; weldability poor	New alloy in U. S.; "good" castability	Good	Good

(a) Temper designations represent expected condition of material after fabrication and heat treatment if any.

A second choice is wrought magnesium. For the spherical covers, AZ31B alloy in the annealed (-0) or partially annealed (-H24) condition is suggested; this would be fabricated by explosive forming (-0 condition) or warm spinning or drawing (-H24 condition), then tempered to the -H24 condition. The flanges should be formed integral with the covers to avoid loss of strength as a result of welding. The center portion could be ring forged and machined or roll forged to dimension if the trunnion lugs are fabricated separately and welded to the center portion; the suggested alloy is AZ80A, which would be aged to the -T5 condition after welding. If the belt is machined from a ring forging with integral trunnion lugs, an alternative material would be ZK60A, aged to the -T5 condition after forging. A suitable casting alloy for this part is QE22A, heat treated to the -T6 temperature.

A third choice and one which is made only because of the relative ease of fabrication is aluminum. The suggested alloy for the spherical covers is 7075 heat treated after forming to the -T6 condition. Casting of the center portion using 356-T61 is recommended.

EXPERIMENTAL EQUIPMENT

In order to duplicate the most severe static loads imposed on the gimbal during operation, a device which subjects the gimbal to linear acceleration was required. The most practical method of meeting this requirement is a spin fixture or centrifuge. When the gimbal is rotated at a fixed distance and speed about an axis, it is subjected to linear acceleration. If the distance is large compared to the shell diameter the variation in acceleration across the shell may be neglected.

Figure 2 shows the device with the experimental gimbal in place. This spin fixture was designed so that the gimbal may be oriented in any position to obtain linear acceleration in any direction.

Electrical-resistance strain gages were used to measure the strains in the gimbal resulting from the inertial loading. Figure 3 shows the location of these strain gages.

The displacements at various points in the gimbal resulting from inertial loads were also recorded. These measurements were made with a linear-variable-differential-transformer (LVDT). Figure 4 shows the gimbal positioned on the spin fixture for acceleration in the -Z direction. The LVDT is shown at the +X trunnion.

Deflections and rotations for the 1-g static-load tests were recorded with 0.0001-inch dial indicators. The rotation or twist was measured with two dial indicators placed a fixed distance apart at the trunnions.

A - Experimental gimbal	F - Spin-fixture base
B - Strain-gage connectors	G - 22-channel slip-ring assembly
C - Strain-gage leads	H - 3-hp motor and variable-speed-drive assembly
D - Adjustable counterweight	I - Miter box
E - Spin-fixture arm	J - Slip clutch

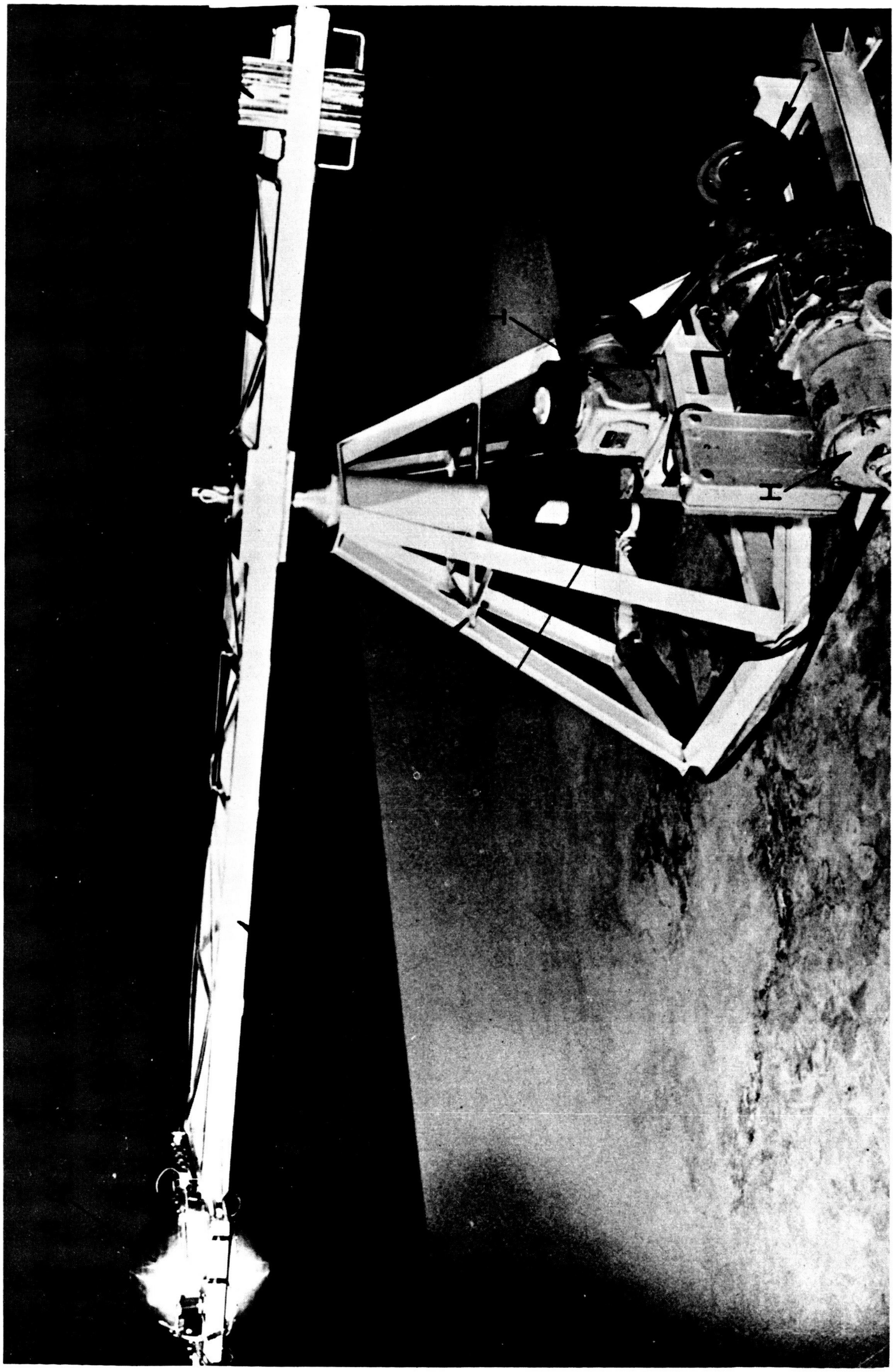

N97751

FIGURE 2. SPIN FIXTURE FOR LINEAR ACCELERATION TESTS

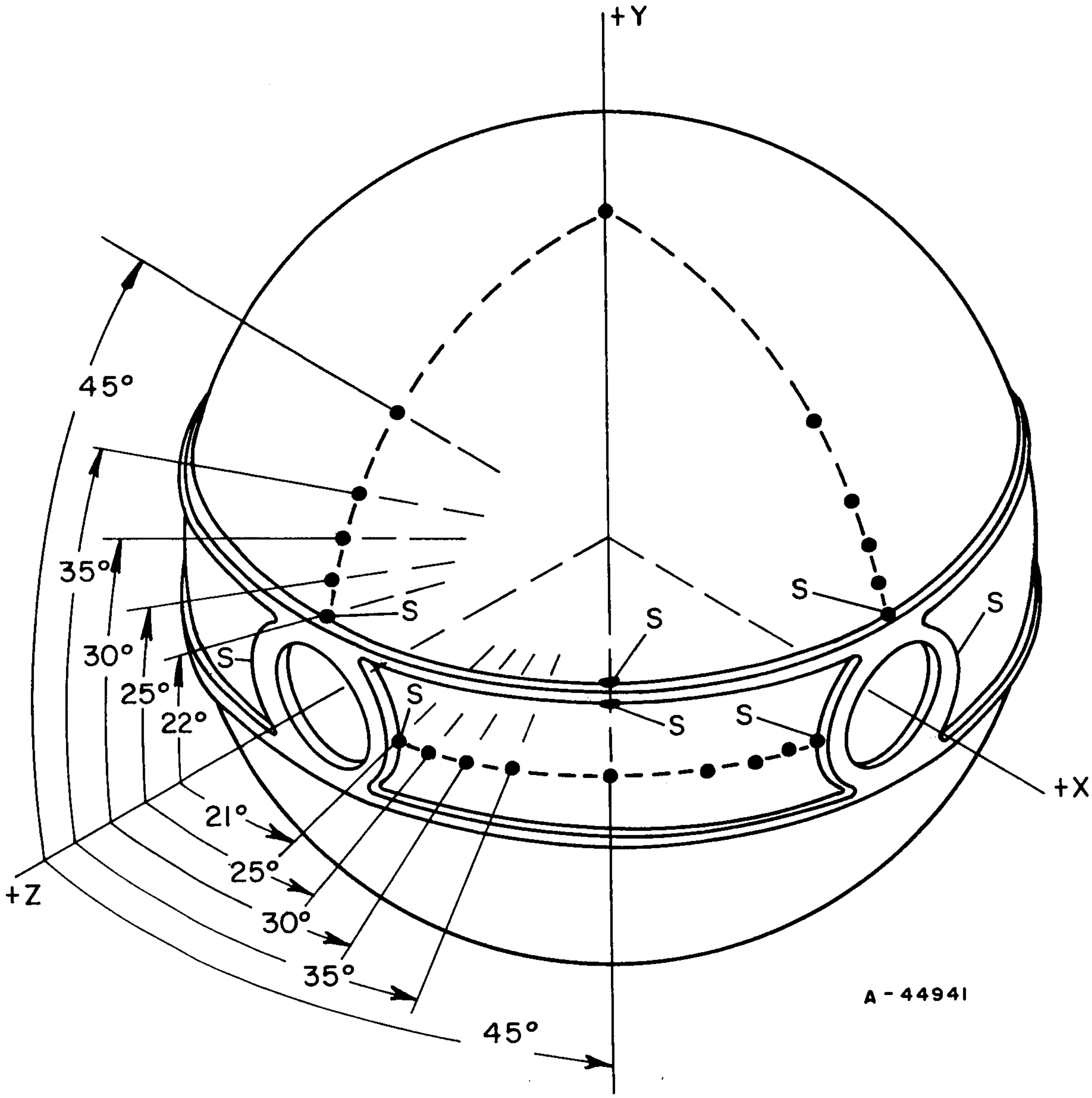

FIGURE 3. STRAIN-GAGE LOCATIONS

S indicates single element strain gage in fillet. All others are 45-degree rosette gages, both inside and outside.

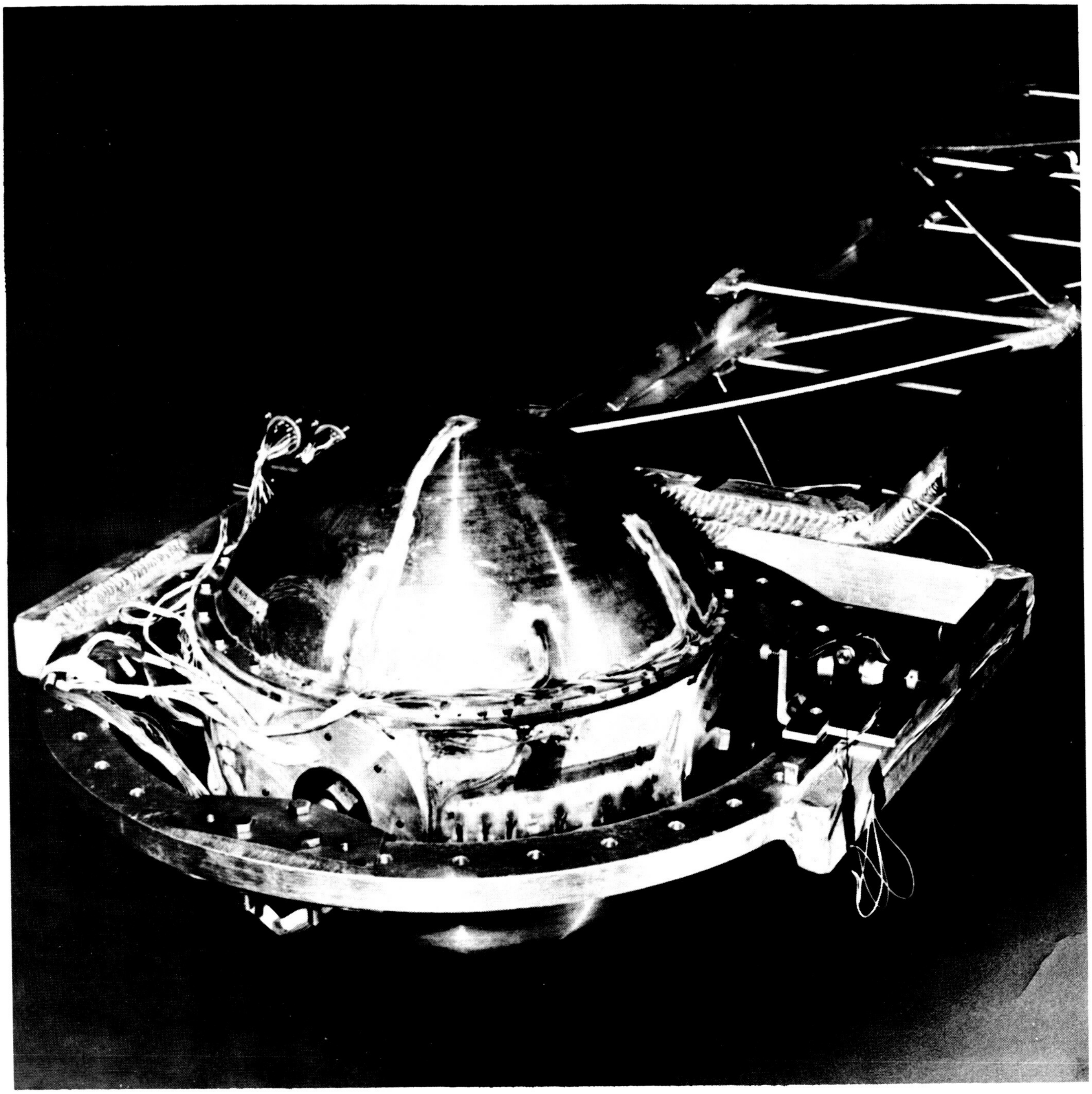

N97748

FIGURE 4. VIEW OF TEST GIMBAL IN PLACE ON THE SPIN FIXTURE

EXPERIMENTAL RESULTS

The dimensions of the experimental gimbal furnished by MSFC are shown in Figures 5 and 6. This gimbal was instrumented with strain gages as shown in Figure 3.

The first series of tests conducted were the linear acceleration tests. The test gimbal was orientated on the spin fixture so that linear accelerations were obtained in turn in each of the three principal directions (X, Y, and Z directions shown in Figure 3). Strains were recorded at all gage locations for an 8-g linear acceleration. These results are presented in Figures 7 through 12. The over-all result of these tests is that strains for these loads are very low and that the bending strains diminish very rapidly as the distance from the flange increases. These bending strains become negligible at about 10 degrees from the flanges in the spherical covers and about 15 degrees in the thicker center section of the spherical gimbal.

These data also indicate that the center section and connecting flanges carry a major portion of the load. Even though the covers are not highly stressed, they do add considerable stiffness to the center section. Static strain readings (loads equivalent to 2 g's) taken with both covers removed and also with them intact dramatically illustrate this stiffening effect. These data are plotted in Figure 13.

A comparison with theoretical results was also made for the strains in the covers when subjected to an axial load at the trunnion (Figures 7 and 9). The theoretical bending strains were obtained by neglecting the flanges (it is believed that the flanges have the least effect on the stresses for this type of loading) and using the curves in Reference (1).* These theoretical bending strains compare favorably with the experimental values. This comparison is shown in Figure 14.

In order for the platform to be initially aligned optically, openings or cutouts are necessary in some of the gimbals. After the maximum size of the cutout required was determined, an opening was made in one of the spherical covers. Figure 15 shows the location and relative size of this opening in the assembled gimbal. After additional strain gages were installed in the neighborhood of the cutout, the gimbal was mounted on the spin fixture and subjected to an 8-g linear acceleration. Figure 16 shows the experimental setup for the 8-g acceleration tests. The resulting strain data were compared to the strain data from the tests conducted before the cutout was made. This comparison of the bending strains in the complete cover is shown in Figures 17 and 18. The strains along the edge of the cover were also recorded. These data are shown in Figure 19. The over-all result is that the cutout produces a small but tolerable increase in the strain levels over the major portion of the gimbal. The maximum strain recorded was 250×10^{-6} inches per inch (2500 psi). This strain occurred in the fillet near the edge of the cutout. Increasing the radius of the fillet at this point and reducing the sharpness of the cutout will decrease this strain.

The deflections recorded during these linear acceleration tests are shown in Table 3.

---

*Page 36.

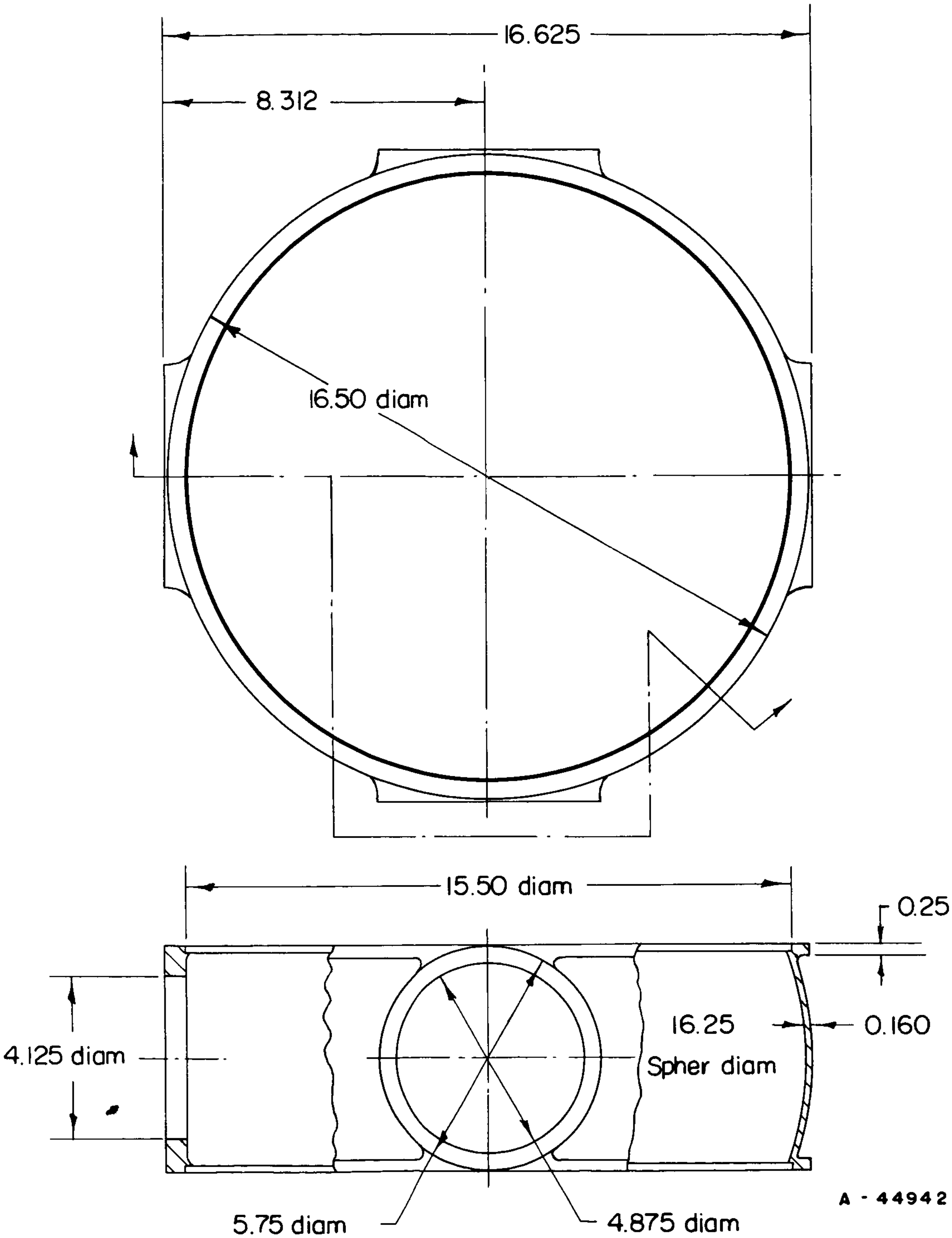

FIGURE 5. DETAILS OF CENTER PORTION OF EXPERIMENTAL GIMBAL

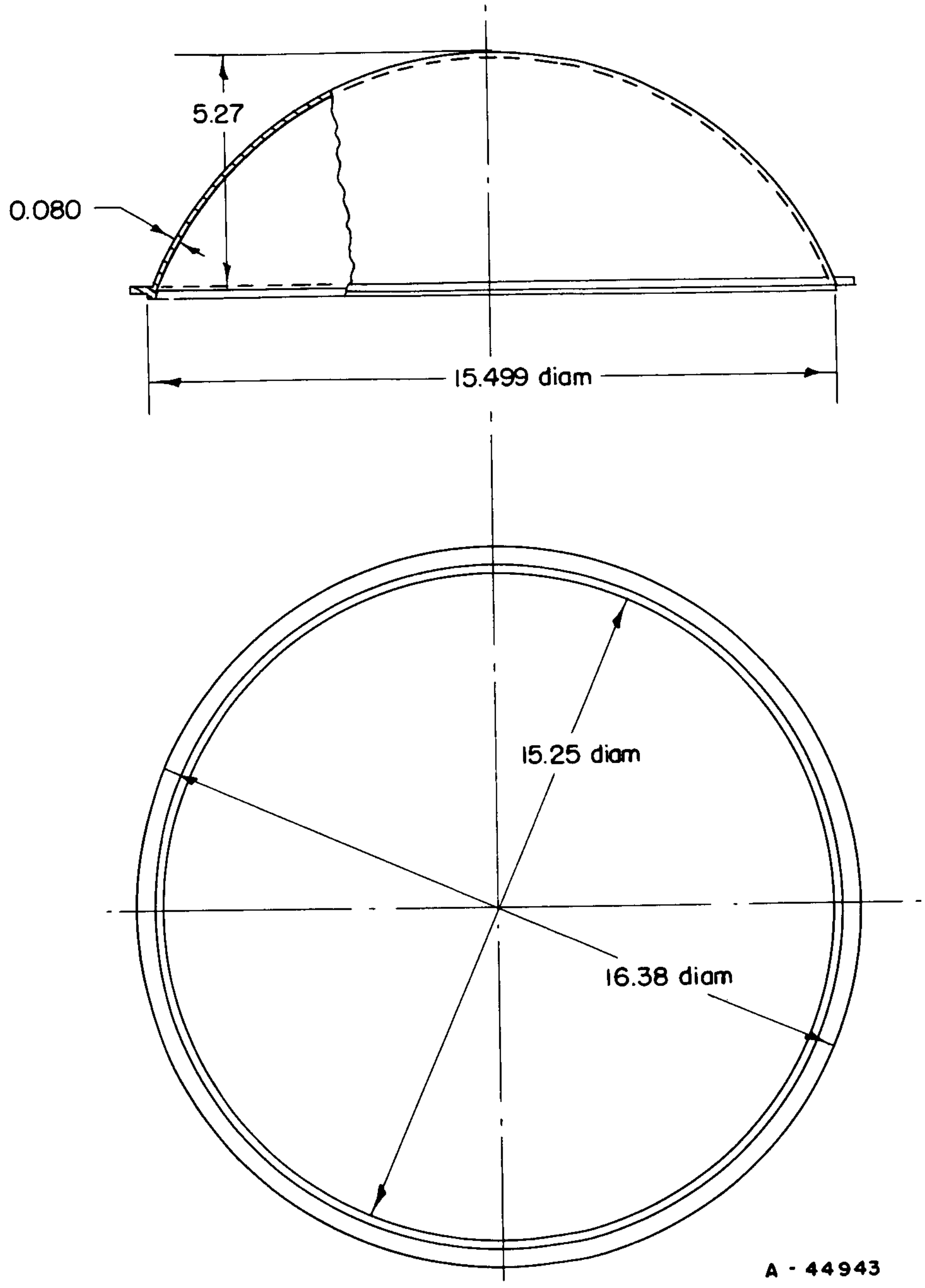

FIGURE 6. DETAILS OF SPHERICAL COVERS OF EXPERIMENTAL GIMBAL

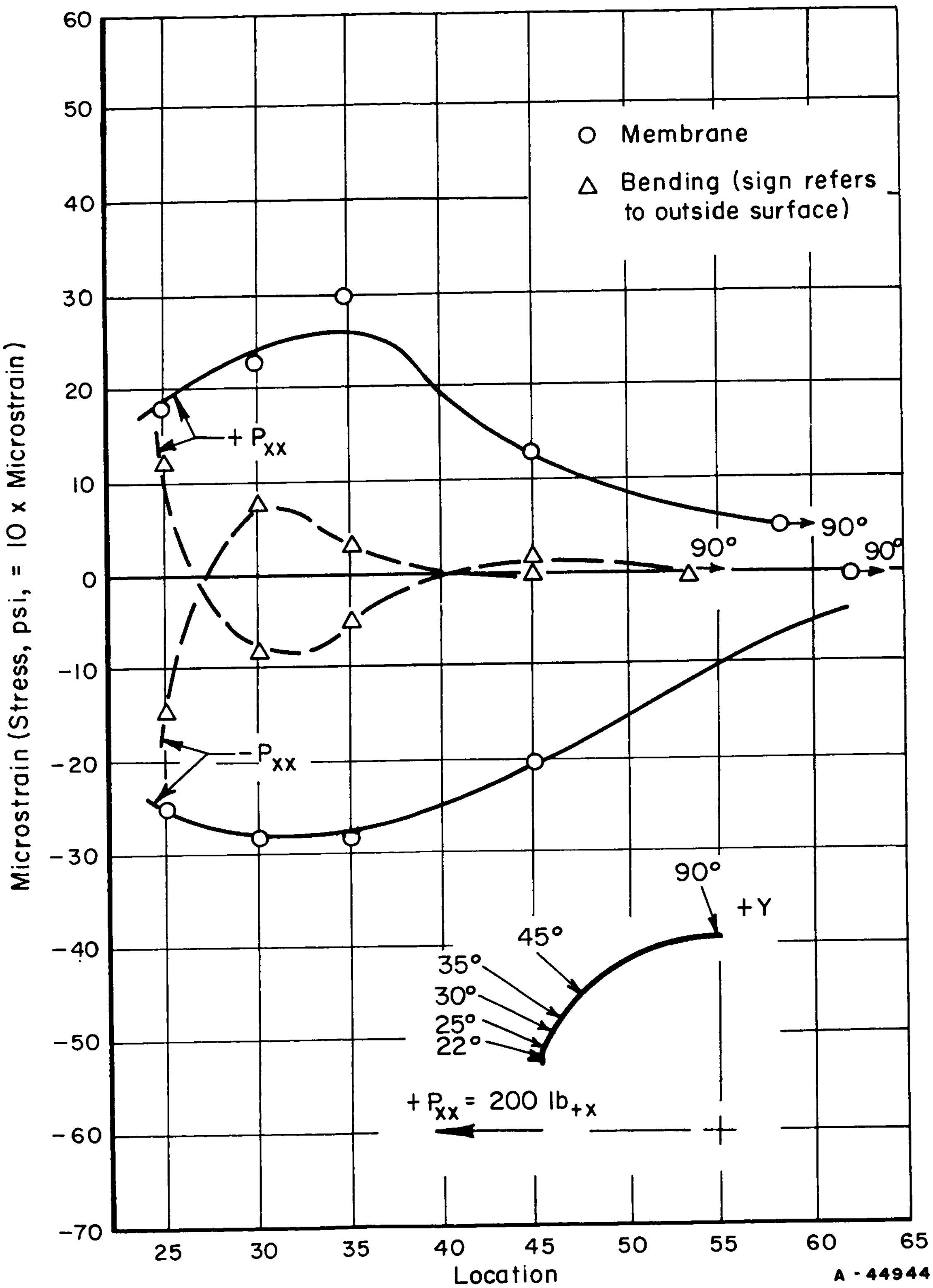

FIGURE 7. STRAINS IN THE SPHERICAL COVERS FOR ±X ACCELERATION (8 G)

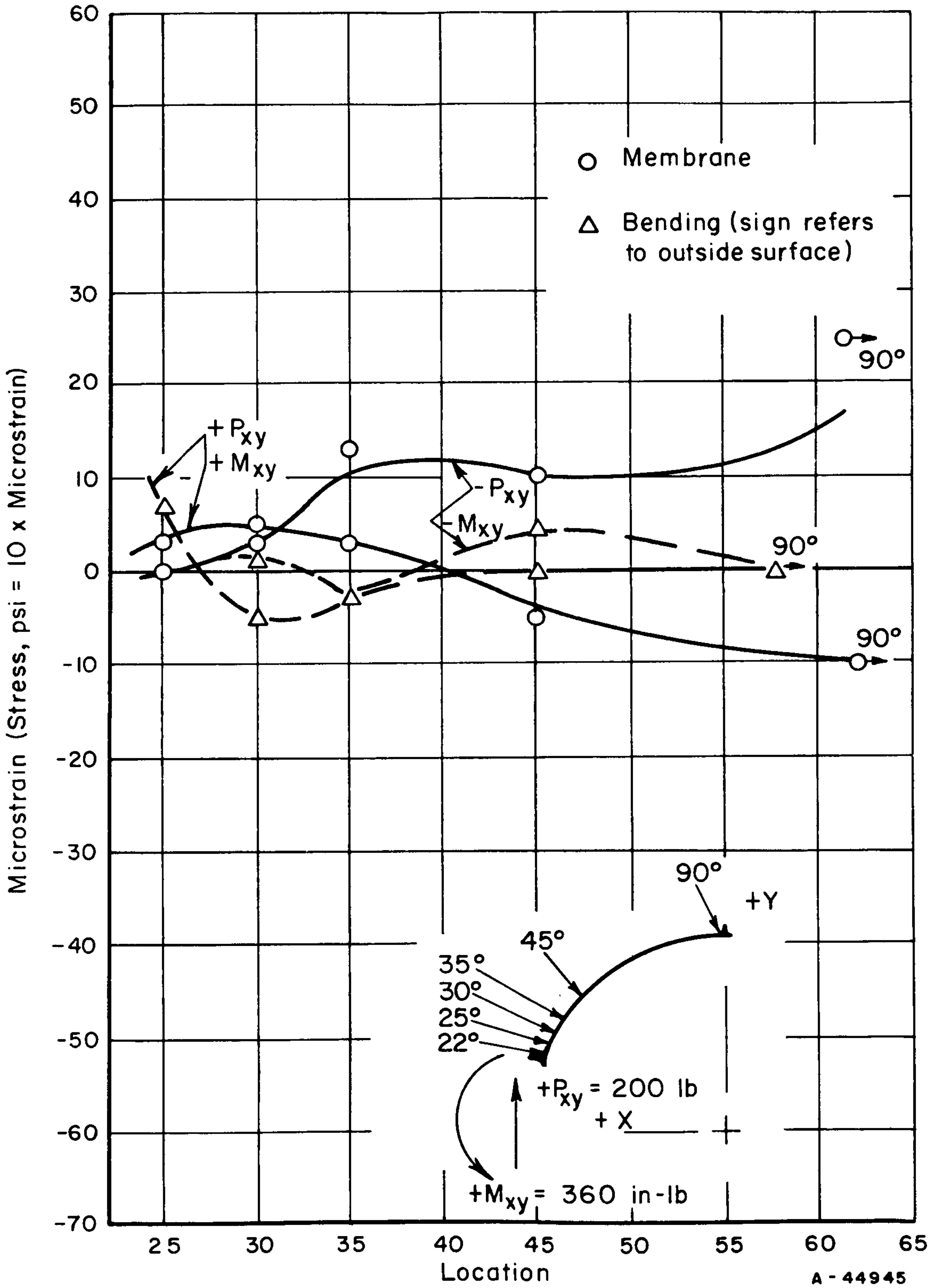

FIGURE 8. STRAINS IN THE SPHERICAL COVERS FOR ±Y ACCELERATION (8 G)

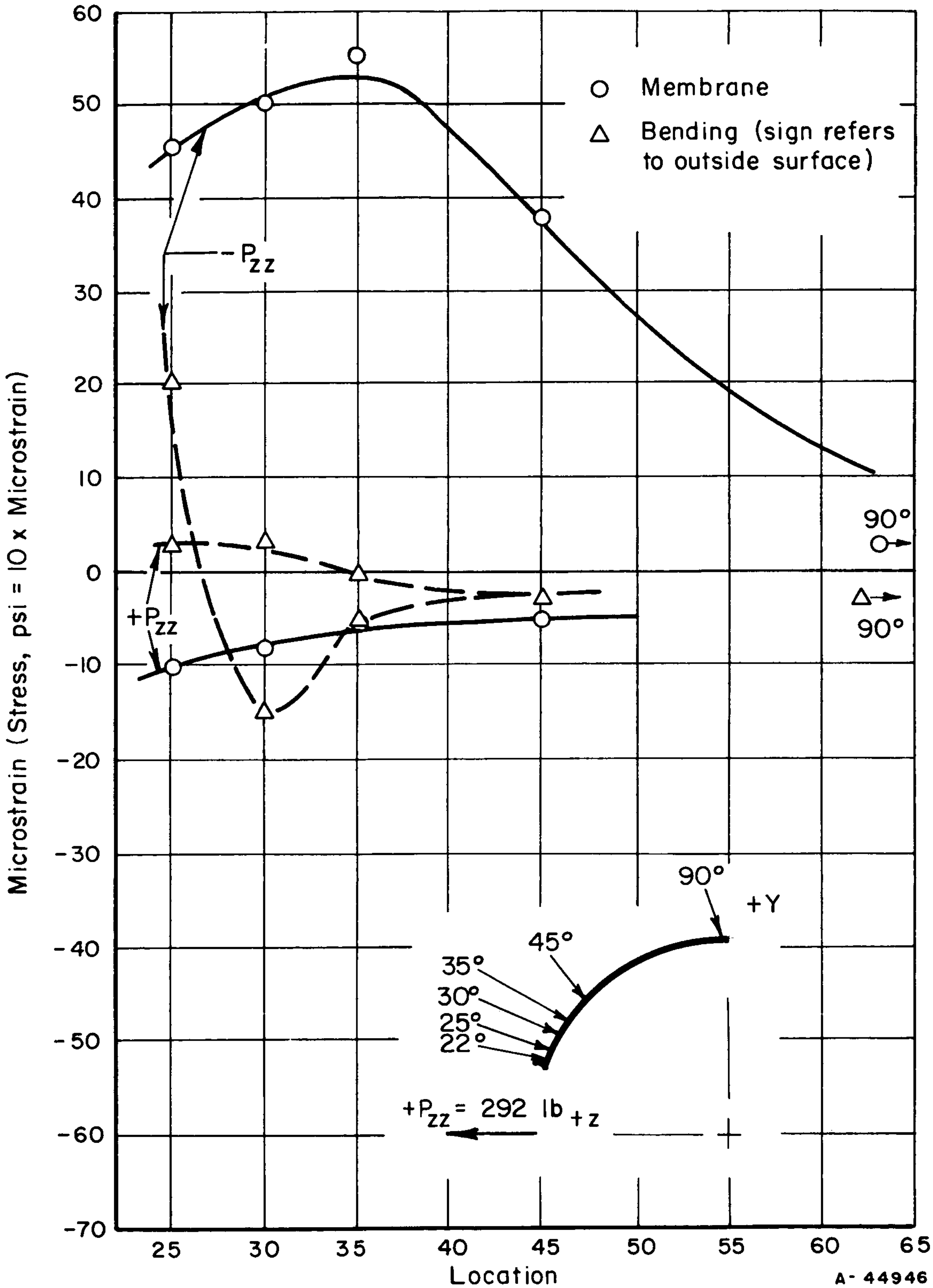

FIGURE 9. STRAINS IN THE SPHERICAL COVERS FOR ±Z ACCELERATION (8 G)

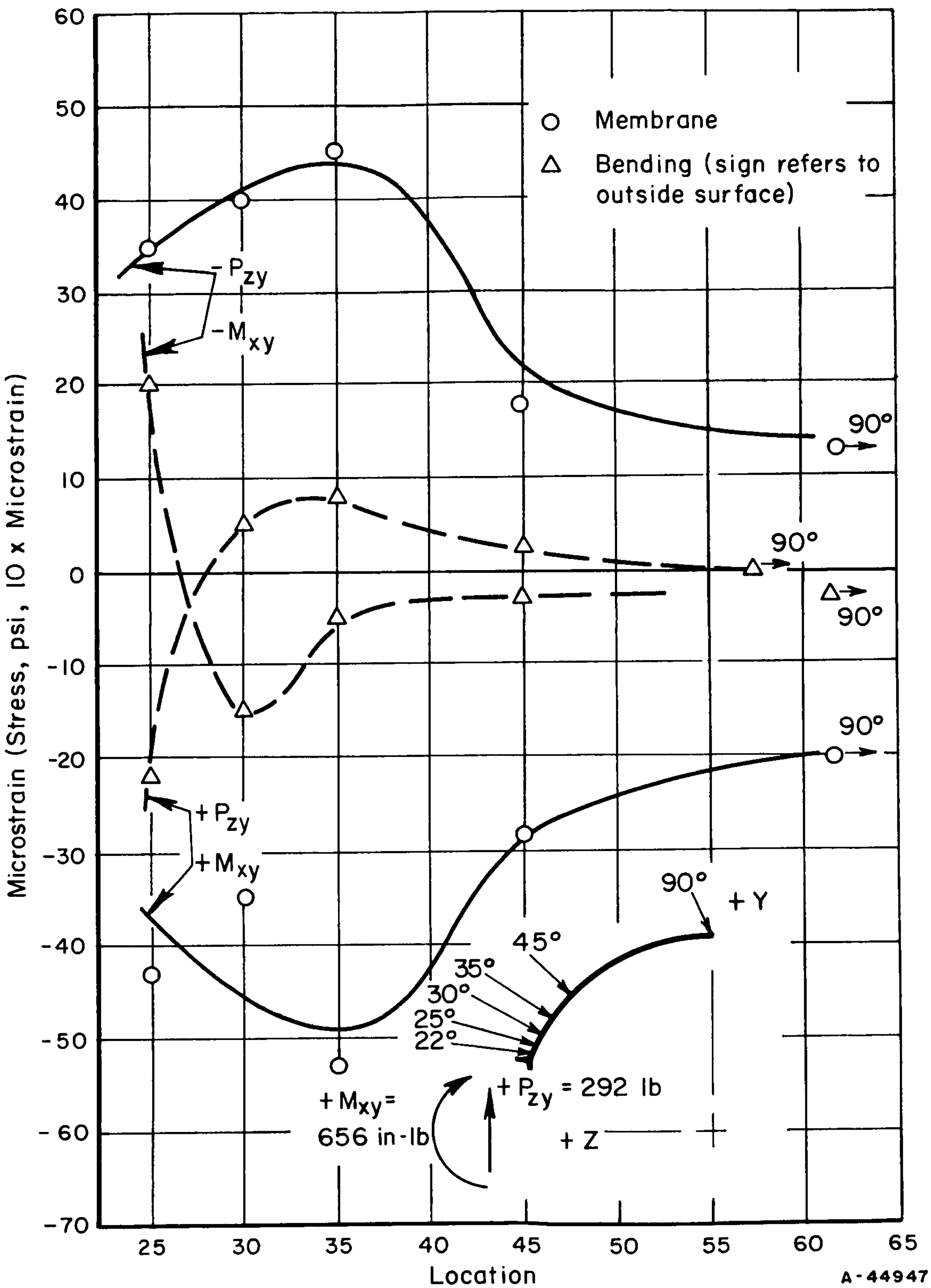

FIGURE 10. STRAINS IN THE SPHERICAL COVERS FOR ±Y ACCELERATION (8 G)

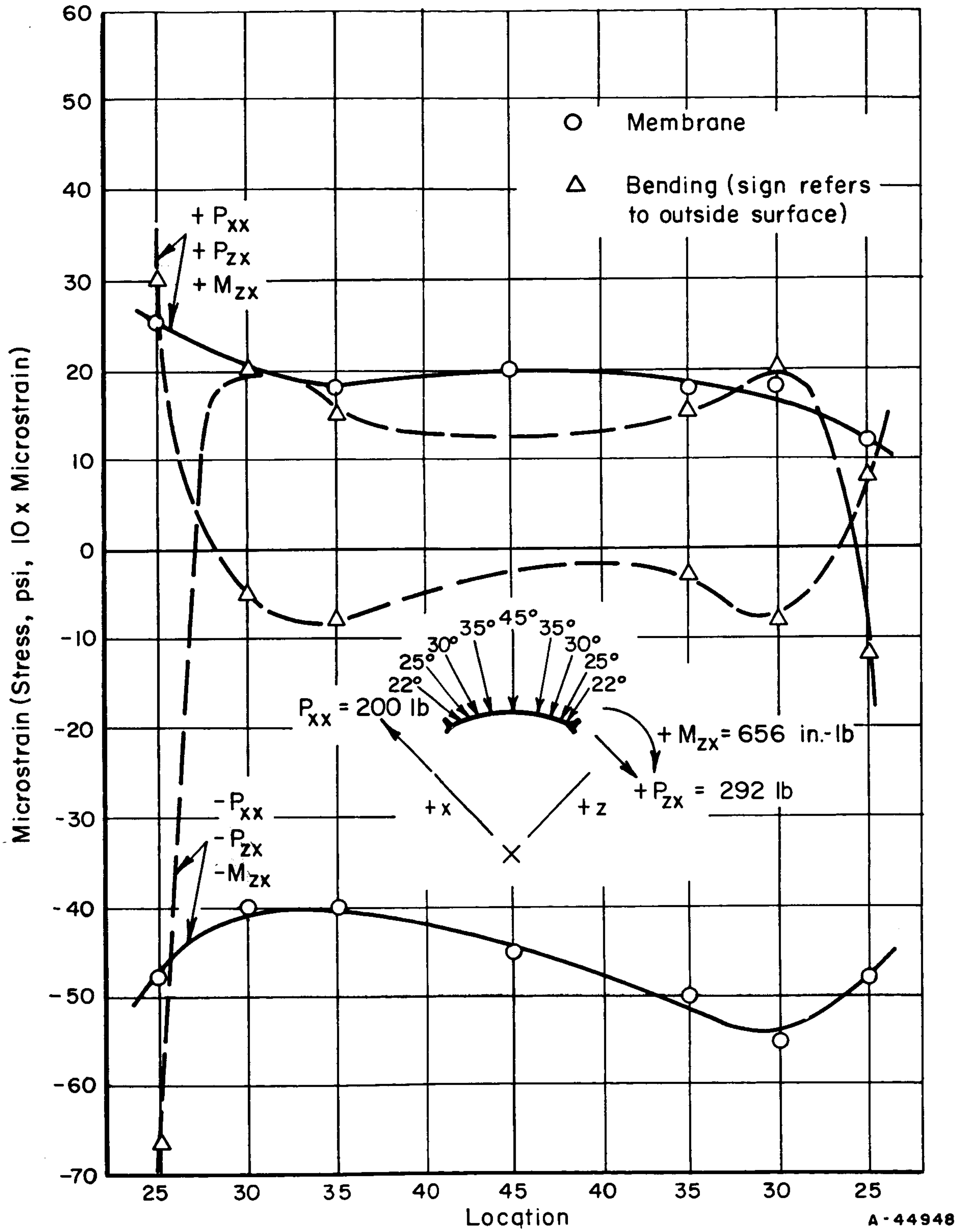

FIGURE 11. STRAINS IN THE CENTER SECTION FOR ±X ACCELERATION (8 G)

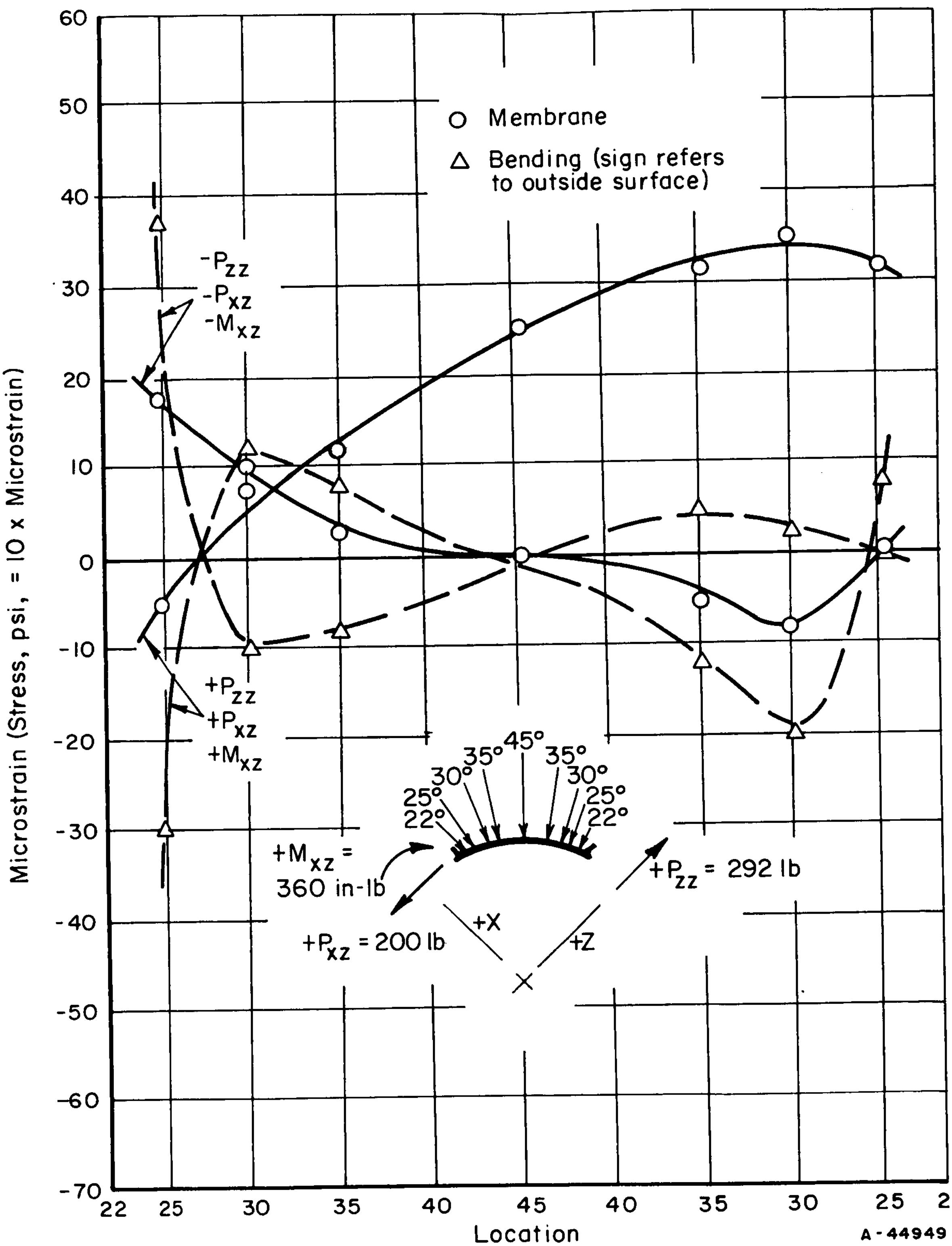

FIGURE 12. STRAINS IN THE CENTER SECTION FOR ±Z ACCELERATION (8 G)

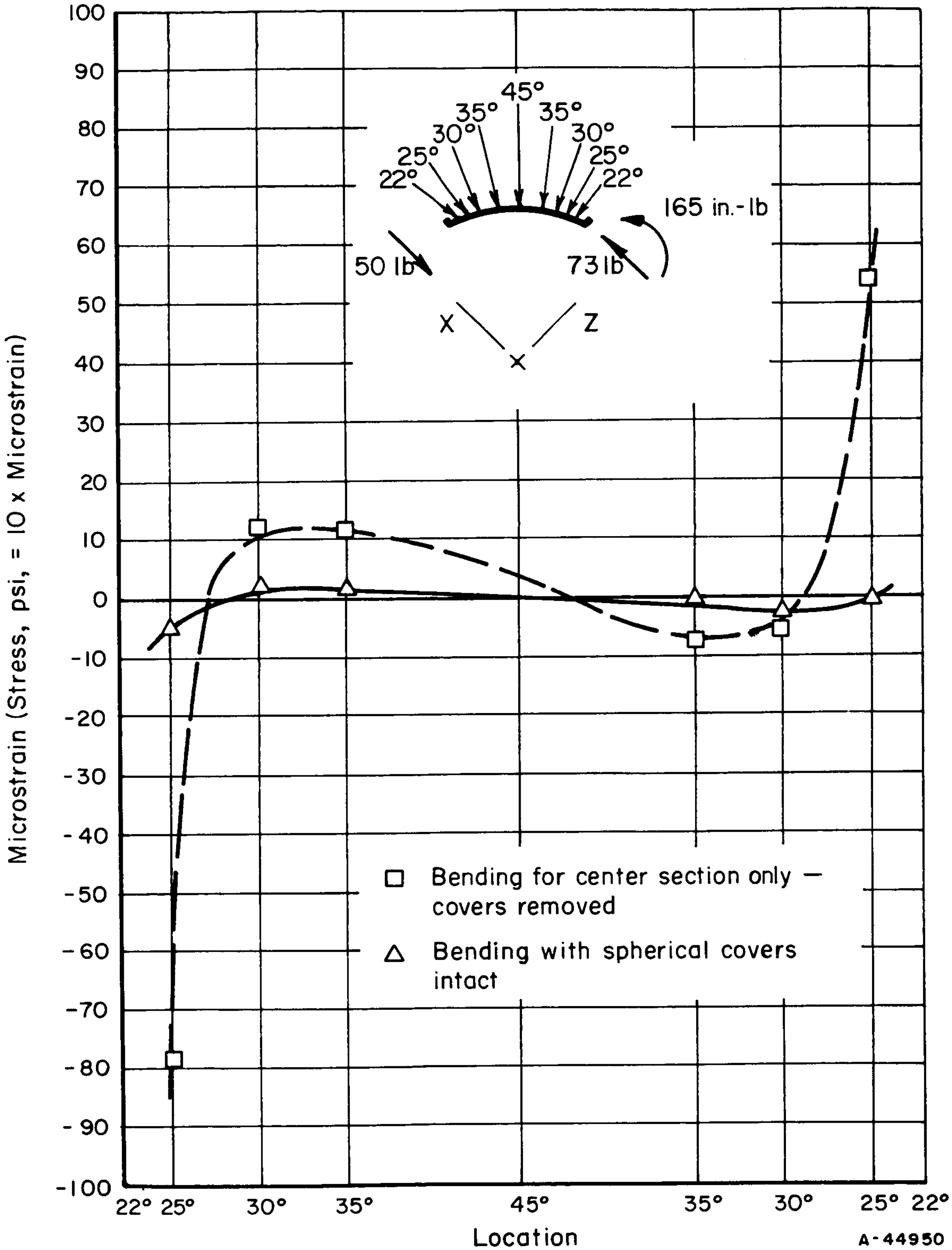

FIGURE 13. BENDING STRAINS IN THE CENTER SECTION FIRST WITH THE SPHERICAL COVERS REMOVED AND THEN WITH THE SPHERICAL COVERS INTACT (2-G LOAD IN -X DIRECTION)

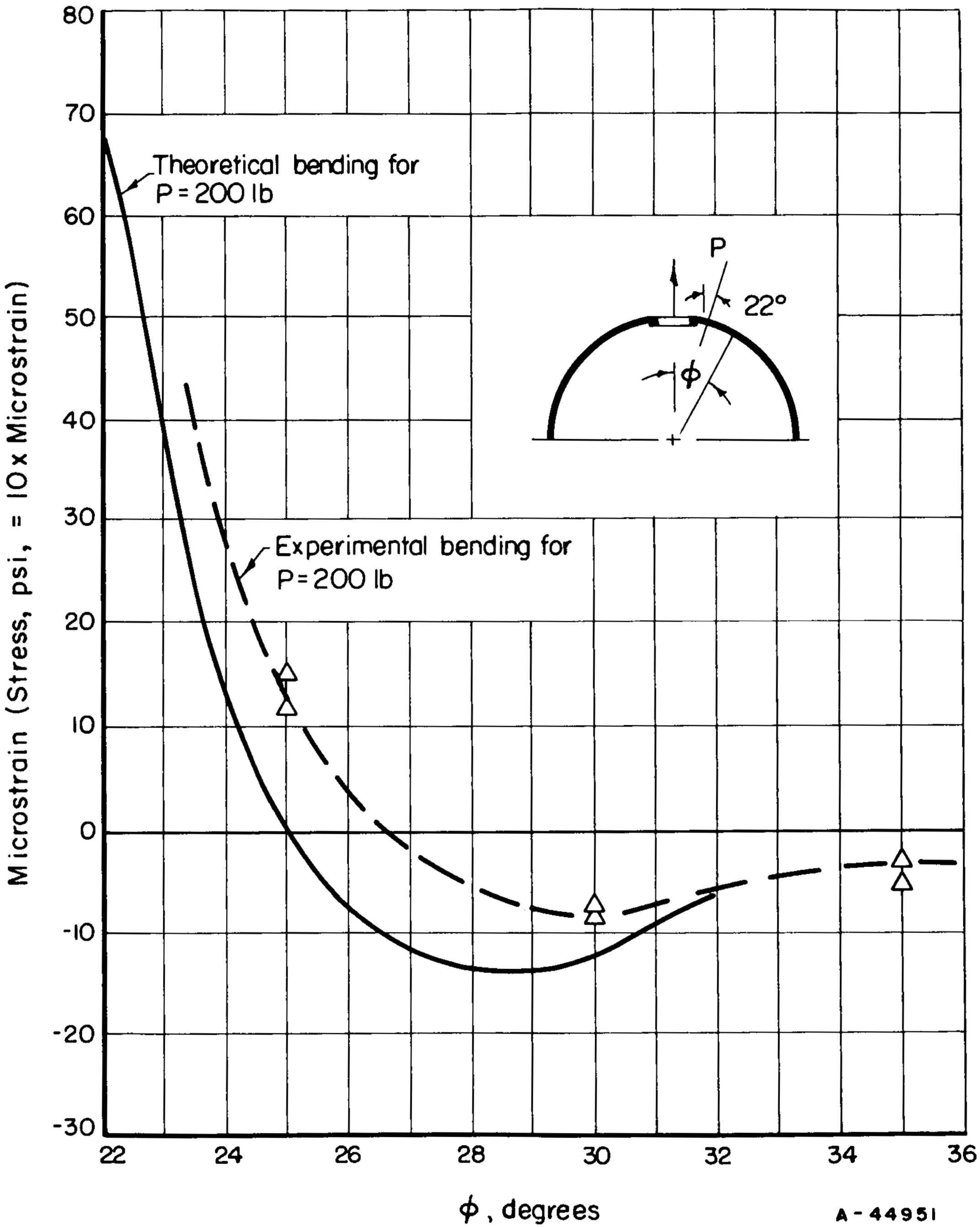

FIGURE 14. A COMPARISON OF THE EXPERIMENTAL BENDING STRAINS WITH THEORETICAL VALUES

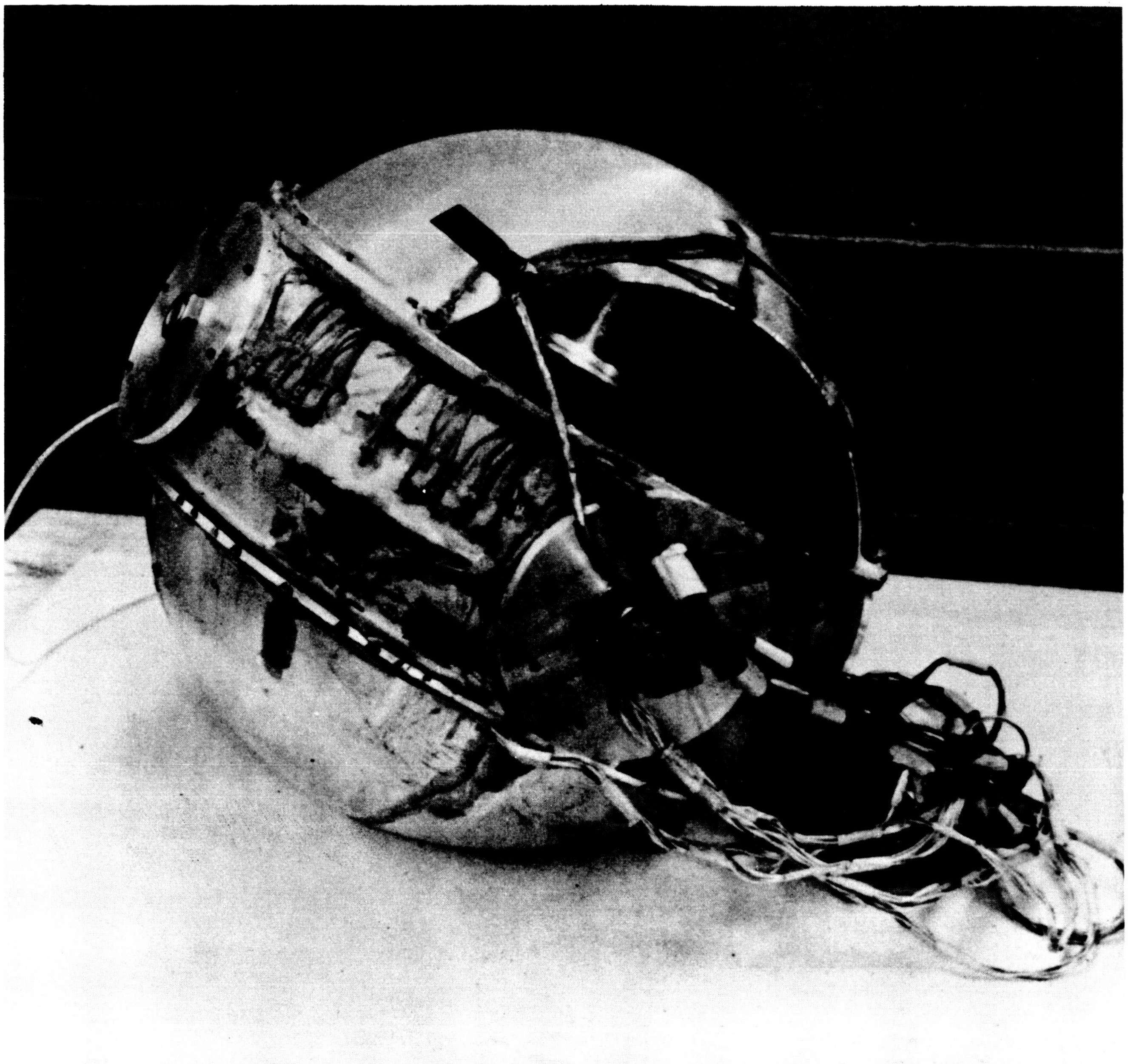

N99305

FIGURE 15. EXPERIMENTAL GIMBAL WITH CUTOUT FOR OPTICAL ALIGNMENT

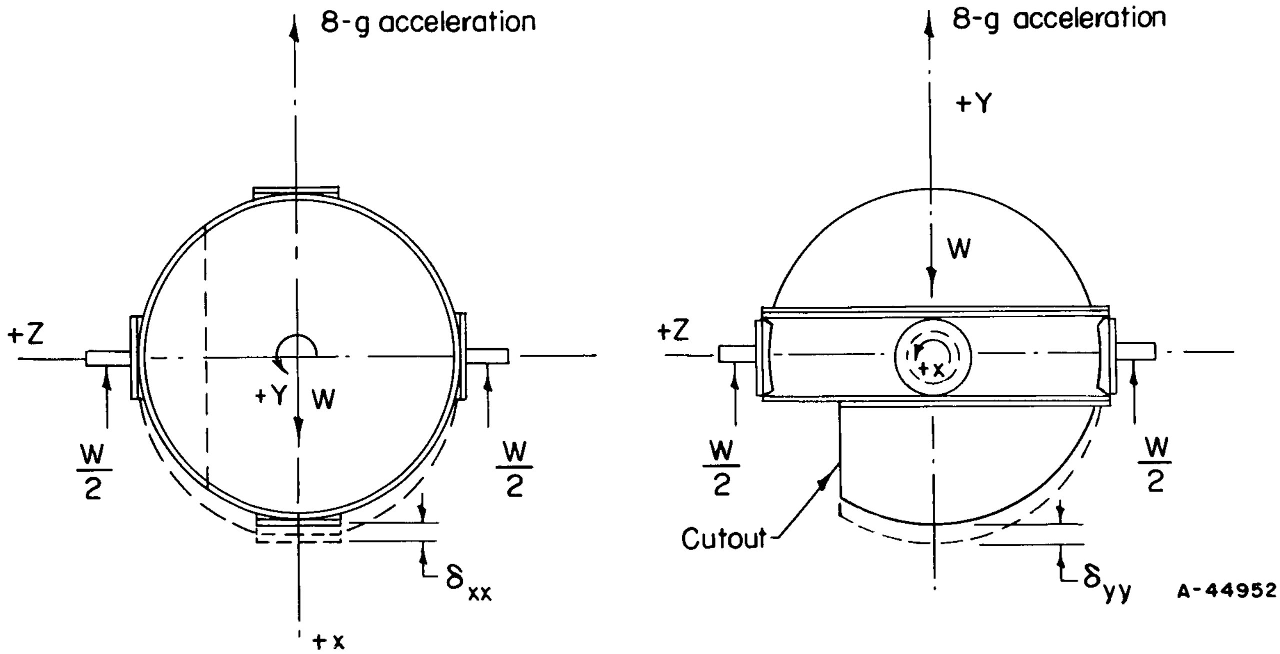

FIGURE 16. EXPERIMENTAL SETUP FOR 8-G INERTIAL LOADING

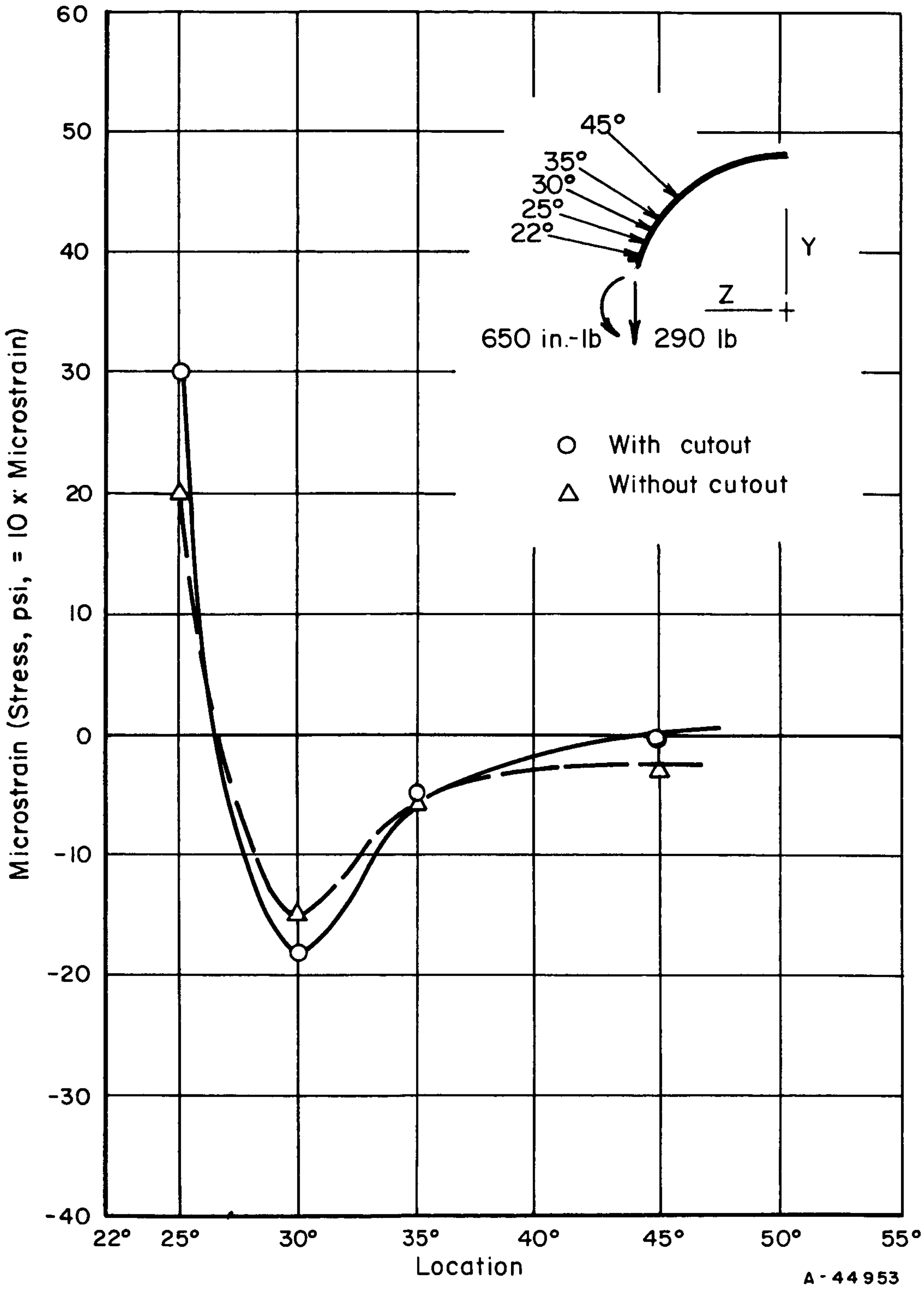

FIGURE 17. COMPARISON OF BENDING STRAINS IN THE SPHERICAL END CAP FOR AN 8-G INERTIAL LOAD IN THE +Y DIRECTION

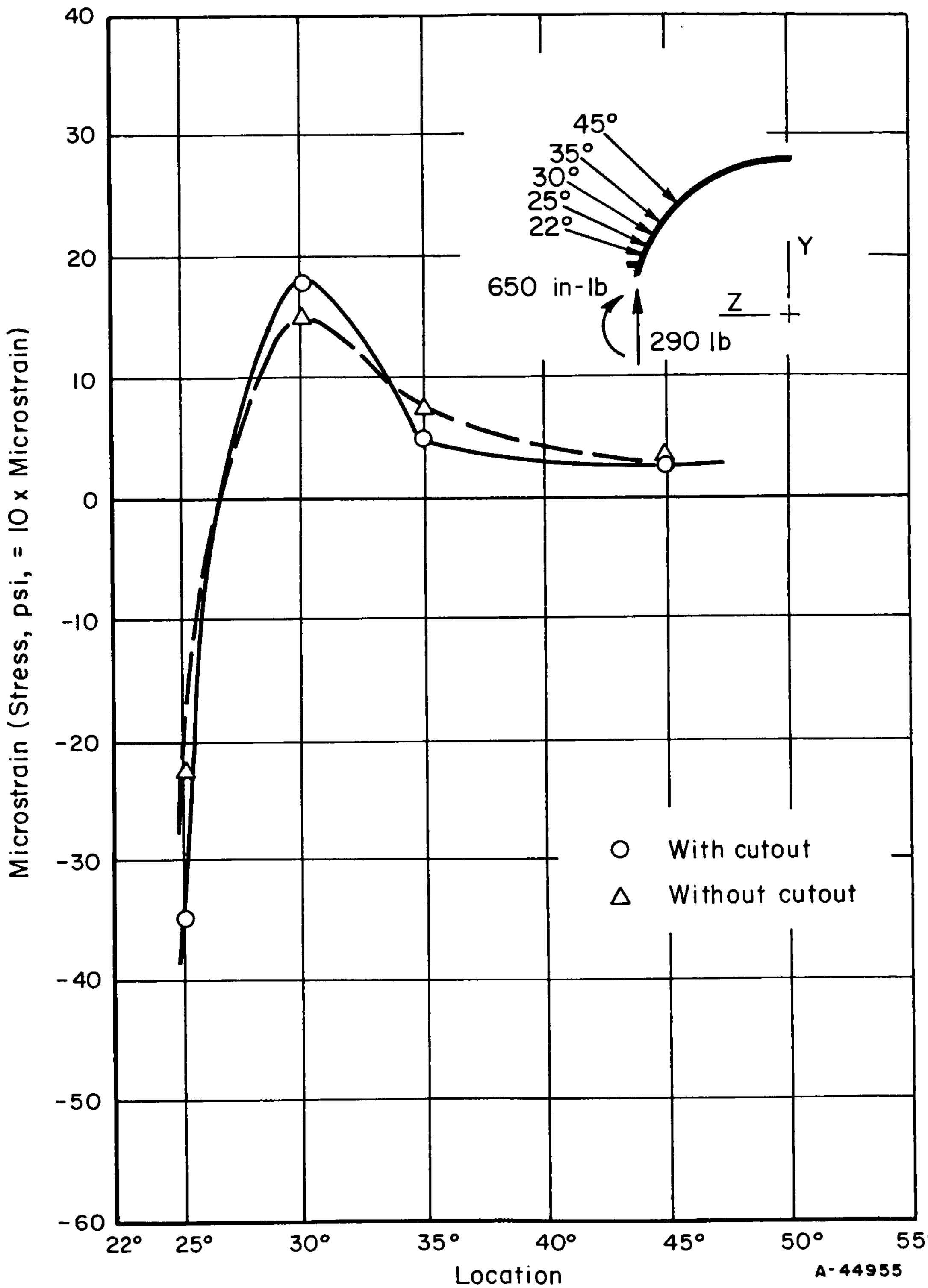

FIGURE 18. COMPARISON OF BENDING STRAINS IN THE SPHERICAL END CAP FOR AN 8-G INERTIAL LOAD IN THE -Y DIRECTION

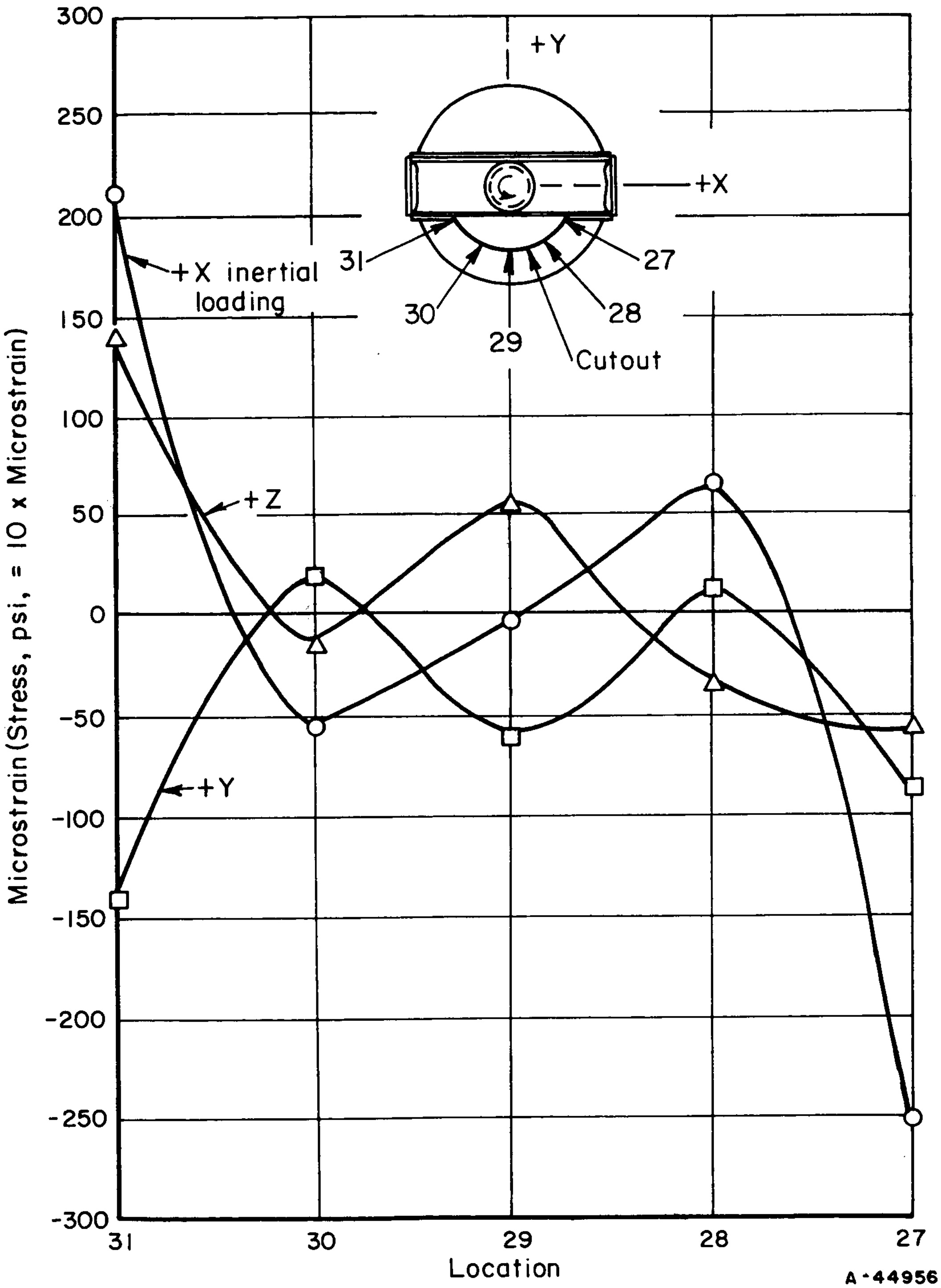

FIGURE 19. STRAINS ALONG THE EDGE OF THE CUTOUT (MEASURED ON THE OUTSIDE SURFACE) FOR INERTIAL LOADS IN THE +X, +Y, AND +Z DIRECTIONS

TABLE 3. DEFLECTIONS DURING 8-G ACCELERATION

	δ_{XX}, inch	δ_{YY}, inch
Complete Gimbal	0.0034	0.0016
With Cutout	0.0031	0.0036

After the linear acceleration tests were completed, static deflection tests were conducted to determine the amount of deflection and misalignment that will be encountered during assembly. Figure 20 shows the experimental setup for these tests. Table 4 shows the magnitude of these quantities as determined from the tests. As seen in this table, the addition of one cap adds considerable stiffness to the gimbal. Relative displacements were also measured during assembly and disassembly of the gimbal (also shown in Table 4). These measurements indicate that the alignment of the trunnions returns to approximately its original position when the gimbal is reassembled. It was later determined, however, that relatively high strains (250 microinches) were induced into the cover due to assembly. These strains are primarily a result of misalignment between the cover and center section. The flatness of the center-section flange was found to vary within the limits of ±0.0004, while the flatness of the cover flange varied ±0.0075 inches. Figure 21 shows the variation in these mating surfaces. It is believed that these tolerances can be much closer in the final assembly, thereby reducing the assembly stresses and misalignments.

TABLE 4.

	θ_Z(a) at Cutout, Radians	θ_Z(a) Opposite Cutout, Radians	θ_X(a), Radians	δ_{XX}(b), inch
Deflections and Twist at Trunnions Under a 1-G Static Load				
For Center Section Only (Figure 20a)	--	0.0012 (4 min 8 sec)	0.0008 (2 min 44 sec)	0.0062
With One Cover Removed (Figure 20b)	--	0.00003 (6 sec)	0.00015 (31 sec)	0.0014
Complete Gimbal (Figure 20c)	0.00007 (14 sec)	0.00002 (4 sec)	0.00006 (12 sec)	0.0016
Misalignment From Repeated Assembly and Disassembly				
Assembled	--	--	0 (reference)	0
Disassembled	--	--	0.00070 (2 min 26 sec)	0.0060
Assembled	--	--	0.00006 (12 sec)	--

(a) Estimated accuracy ±15 sec.
(b) Estimated accuracy ±0.0002 inch.

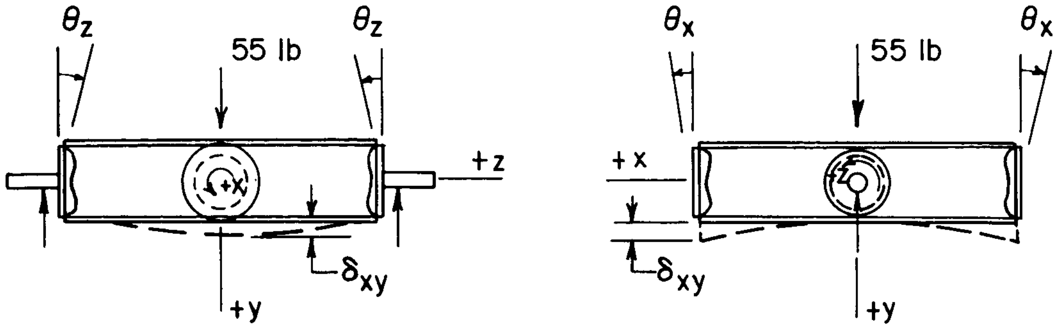

a. Center Section Only — Both Covers Removed

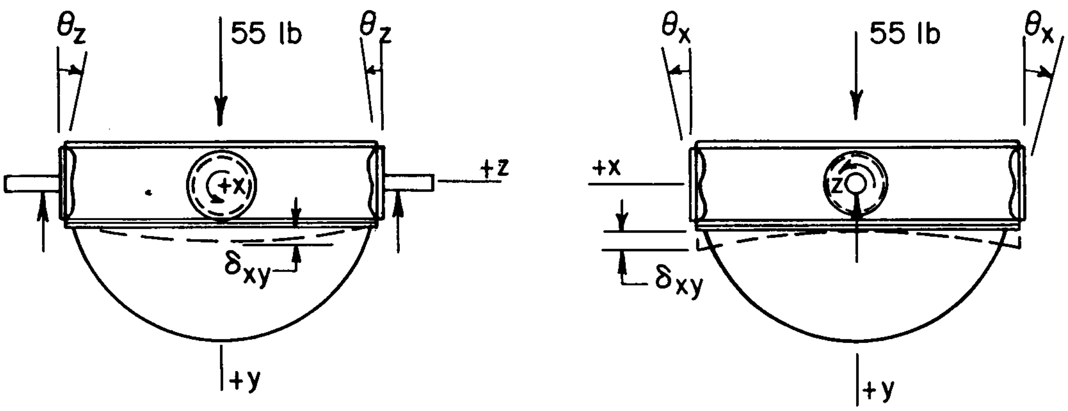

b. With One Cover Removed

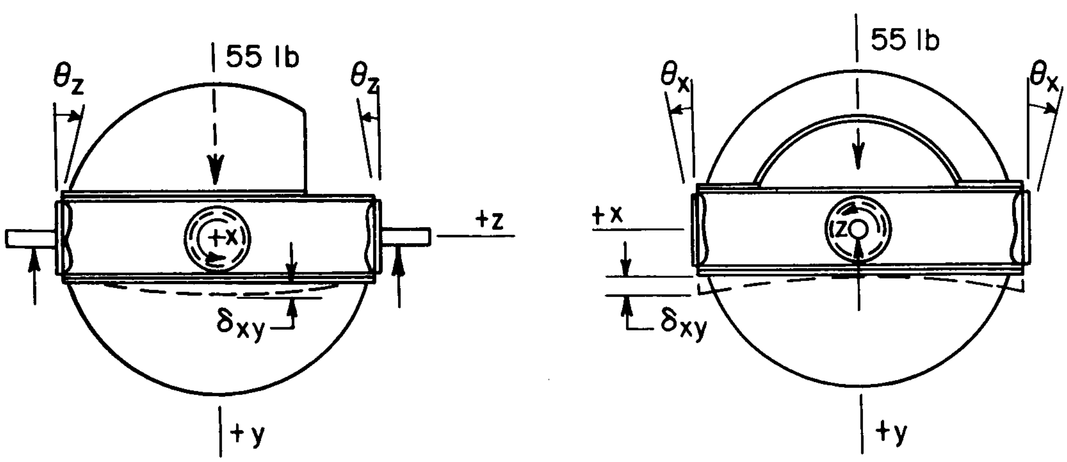

c. Complete Gimbal — Both Covers Intact

A-44957

FIGURE 20. EXPERIMENTAL SETUP FOR STATIC LOAD TESTS

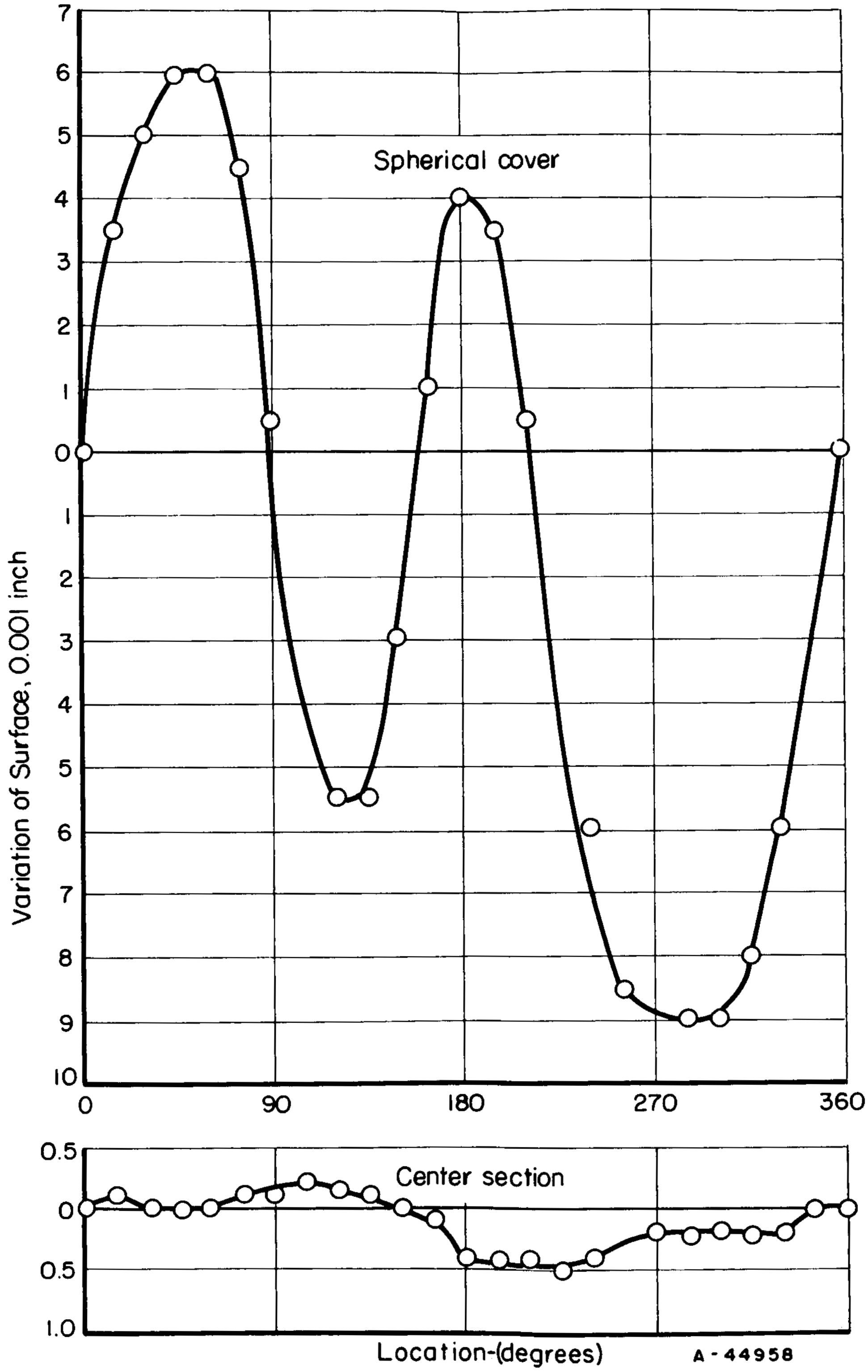

FIGURE 21. VARIATION IN FLATNESS OF THE SPHERICAL COVER FLANGE AND MATING FLANGE ON THE CENTER SECTION

DESIGN MODIFICATIONS

The results of these experiments show that the strains for an 8-g linear acceleration are very low. This would indicate that the thickness of this gimbal can be substantially reduced without exceeding the strength limits of the material. The equation for the meridional stress at any point in the gimbal is:

$$\sigma_\phi = \frac{6\ M_\phi}{t^2} + \frac{N_\phi}{t} \quad , \tag{1}$$

where

M_ϕ = meridional bending moment $\frac{\text{in-lb}}{\text{in.}}$

N_ϕ = meridional membrane force $\frac{\text{lb}}{\text{in.}}$

t = thickness of shell, inches.

Using the experimental strain data to determine M_ϕ and N_ϕ:

$$M_\phi = \frac{t^2}{6}\ \epsilon_b\ E$$

$$N_\phi = t\ \epsilon_d\ E$$

where

ϵ_b = bending strain

ϵ_d = membrane strain

E = modulus of elasticity.

For the spherical covers:

$$t = 0.080 \text{ inch}$$

$$E = 10 \times 10^6 \text{ psi.}$$

$$\therefore\ M_\phi = \frac{(0.08)^2 \times 10}{6}\ \epsilon_b \times 10^6$$

$$= 0.01068\ \epsilon_b \times 10^6 \text{ and} \tag{2}$$

$$N_\phi = 0.80\ \epsilon_d \times 10^6. \tag{3}$$

The maximum values of ϵ_b and ϵ_d measured at each point and the resulting values of M_ϕ and N_ϕ as determined from Equations (2) and (3) are:

ϕ, degrees	ϵ_b, microinches	ϵ_d, microinches	M_ϕ, in-lb/in.	N_ϕ, lb/in.
22	70[(a)]	45[(a)]	0.75	36
25	22	45	0.24	36
30	15	50	0.16	40
35	8	55	0.09	44
45	5	38	0.05	30

(a) Extrapolated from strain data.

Using a design stress of 4000 psi, and solving for t from Equation (1), the required thickness profile for the redundant gimbal cover is:

ϕ, degrees	Thickness (t), inch
22	0.0383
25	0.0240
30	0.0214
35	0.0184
45	0.0132

If the strength were the only consideration, this would be the required thickness profile. However, stiffness and fabricability of the material are also important factors in this design. Because of these considerations, a minimum thickness of 0.040 inch for the spherical covers is recommended. To fabricate these spherical covers to the required tolerances from materials with thicknesses less than 0.040 inch would be very difficult.

For the center section, the maximum strains and resulting bending moments and membrane forces are:

ϕ, degrees	ϵ_b, microinches	ϵ_d, microinches	M_ϕ, in-lb/in.	N_ϕ, lb/in.
22	150[(a)]	50[(a)]	6.40	80
25	67	48	2.86	80
30	20	55	0.85	80
35	15	50	0.64	80
45	15	50	0.64	80

(a) Extrapolated from strain data.

Again, using an allowable stress of 4000 psi, the required thickness profile is [using Equation (1)]:

ϕ, degrees	Thickness (t), inch
22	0.1085
25	0.0764
30	0.0471
35	0.0425
45	0.0425

Here again, stiffness and fabricability must also be considered. Note, however, that in order to keep the stress below 4000 psi, a thickness of 0.1085 inch is required at ϕ = 22 degrees. This is at the junction of the heavier trunnion section and thinner spherical section. If a 1/2-inch fillet radius is used at this junction, the actual thickness at this point will be greater than the thickness of the spherical section. This 1/2-inch fillet will extend slightly beyond ϕ = 25 degrees, where the required thickness is 0.0764 inch. Therefore, a thickness of 0.080 inch is recommended for the center section of the redundant gimbal.

The stresses not only depend on the magnitude of the loads but on the D/t (diameter-to-thickness) ratio of the gimbal. As the D/t ratio decreases, the stresses will decrease in magnitude for the same load.

Therefore, in order to extrapolate the strain data from these experiments to smaller gimbals, both the decrease in load and D/t ratio must be considered. This type of an analysis would result in thicknesses less than that determined for the redundant gimbal. Because the thickness of the redundant-gimbal covers is already at a minimum value, the analysis would not yield significant results. Therefore, a thickness of 0.040 inch is recommended for the outer- and middle-gimbal covers. This same type of approach can be used to determine the thickness of the center sections. For the center section, however, the thickness may be reduced from the 0.080-inch value. A thickness of 0.060 inch (probable minimum for casting and machining) is recommended for the outer- and middle-gimbal center section.

This investigation showed that the flanges carried a major portion of the load. In order to stiffen the center section and eliminate the rather sharp re-entrant corner at the junction of the flange and spherical section, a larger fillet radius is recommended at this point. It is also important to have a relatively stiff center section to minimize the deflections and misalignments encountered during repeated assembly and disassembly of the gimbal. This is another reason for having the center section thicker than the covers.

(The experimental data developed in this project are recorded in Battelle files and Laboratory Record Book No. 19958.)

REFERENCE

(1) Steele, C. R., "Nonsymmetric Deformation of Dome-Shaped Shells of Revolution", J. Appl. Mech., 29 (2), Series E, 353-361 (June, 1962).

JES:TJA:GMM/ng